Stabilized Spin-Polarized Jellium Model and Odd-Even Alternations in Jellium Metal Clusters

M. Payami and N. Nafari

Center for Theoretical Physics and Mathematics, P. O. Box 11365-8486, Tehran, Iran; and

International Center for Theoretical Physics, P. O. Box 586, 34100 Trieste, Italy (September 15, 2018)

Abstract

In this paper, we have considered the mechanical stability of a jellium system in the presence of spin degrees of freedom and have generalized the stabilized jellium model, introduced by J. P. Perdew, H. Q. Tran, and E. D. Smith [Phys. Rev. B 42, 11627 (1990)], to a spin-polarized case. By applying this generalization to metal clusters (Al, Ga, Li, Na, K, Cs), we gain additional insights about the odd-even alternations, seen in their ionization potentials. In this generalization, in addition to the electronic degrees of freedom, we allow the positive jellium background to expand as the clusters' polarization increases. In fact, our self-consistent calculations of the energetics of alkali metal clusters with spherical geometries, in the context of density functional theory and local spin density approximation, show that the energy of a cluster is minimized for a configuration with maximum spin compensation (MSC). That is, for clusters with even number of electrons, the energy minimization gives rise to complete compensation $(N_{\uparrow} = N_{\downarrow})$, and for clusters with odd number of electrons, only one electron remains uncompensated $(N_{\uparrow} - N_{\downarrow} = 1)$. It is this MSC-rule which gives rise to alternations in the ionization potentials. Aside from very few exceptions, the MSC-rule is also at work for other metal culsters (Al, Ga) of various sizes.

36.40, 71.10, 31.15.E

Typeset using $\text{REVT}_{\text{E}}X$

I. INTRODUCTION

The subject of metal clusters has gained considerable momentum in recent years¹⁻⁶. The first step for studying these systems, has been to employ the spherical jellium model (JM) along with the density functional formalism $(DFF)^{7-10}$. However, the spherical-JM despite its initial successes suffers from two main deficiencies.

Firstly, the approximation that metal clusters assume spherical geometry, can only be justified for large closed-shell clusters, but not for very small clusters having closed- or open-shell electronic configurations. Therefore, some authors have used the deformed spheroidal- or ellipsoidal-JMs¹¹⁻¹⁸. The results of *ab initio* molecular dynamics calculations¹⁹ confirm the overall shapes predicted by the deformed-JMs. Koskinen and coworkers²⁰ in their ultimate-JM have assumed the jellium background to be completely deformable both in shape and in density. However, the ultimate-JM is applicable only when the local density parameter, r_s , does not differ much from 4.18, i.e., the r_s -value for which the jellium system is in mechanical equilibrium. In the following we will discuss the mechanical stability of the JM.

The second drawback arise from the JM itself. It is well-known that the JM yields negative surface energies²¹ at high electron densities $(r_s \leq 2)$, and negative bulk moduli²² for $r_s \approx 6$. These drawbacks are expected to manifest themselves in the jellium metal clusters too. To overcome these deficiencies, some authors have brought in the ionic structure either perturbatively²¹⁻²⁵ or variationally²⁶⁻²⁸. However, other researchers have tried to modify the JM in such a way as to keep its simplicity and yet avoid the above-mentioned drawbacks²⁹⁻³³. These authors emphasize that the jellium system is not in mechanical equilibrium, except for $r_s \approx 4.18$. In particular, we refer to the work of Perdew, Tran, and Smith³³ who have introduced the stabilized jellium model (SJM). Applications of the SJM to infinite and semi-infinite simple metals^{33,34} yield realistic estimates for the cohesive and surface energies. In fact, the SJM-calculations of the energetics of simple metal clusters with spherical geometries³⁵, and voids³⁶ show an appreciable improvements over the simple JM results. For example, the energy per particle for large sodium metal clusters changes from $\sim -2eV$ to $\sim -6eV$.

However, according to what was mentioned earlier, the spherical-SJM may only be suitable for clusters with closed-shell electronic configurations. The reasons are two-fold: i) In the SJM, the stabilization has been accomplished for a spin-compensated system which is not necessarily suitable for open-shell clusters. ii) The electronic charge densities for open-shell systems do not have spherical symmetry.

Thus, to study open-shell clusters, two modifications over the spherical-SJM need be done. Firstly, open-shell clusters are not generally expected to have zero polarization. This is particularly true for clusters with odd number of valence electrons. Therefore, the SJM must be generalized to the stabilized spin-polarized jellium model (SSPJM) which is the subject of this work. Secondly, because of the deformations due to the Jahn-Teller effect³⁷ for open-shell systems, one should employ deformed nonspherical shapes for the jellium background. Röthlisberger and Andreoni³⁸ by using the Car-Parrinello³⁹ method, i.e., the unified DFF and molecular dynamics, have obtained interesting results. The results of their extensive computer simulation show that on the one hand, the overall shapes of clusters change when the number of atoms in clusters change. This supports the deformed jellium models. On the other hand, they show that the average distance between the nearest neighbors, d_{av} , in sodium microclusters alternate with increasing number of sodium atoms (see Fig. 15 of Ref. [38]). We will show that these alternations are predicted via the SSPJM.

Guided by these results, we have asked whether it is possible, to keep the spherical geometry and further improve the results obtained using the spherical-SJM. Our answer is positive⁴⁰. In fact, in the spherical-SSPJM, by allowing the volume of a cluster change as a function of its spin-polarization, we arrive at new results which are absent in the previous spherical-JM or spherical-SJM and gain further insights for the observed odd-even alternations in the ionization potentials (IP) of metal clusters^{4,41,42}. For clarification purposes, we mention that it is the difference of the level separations near the Fermi level for the neutral and ionized clusters which gives rise to alternations in IPs. These changes can show up: i) By allowing nonspherical shape deformations of the jellium background (JB) while keeping its volume fixed¹¹⁻¹⁸. ii) By preserving the spherical shape of the JB and allowing its volume per valence electron change. The latter is what we are addressing in this paper. We will see that the mechanism causing changes in the JB volume is rooted in the stabilization of the spin-polarized JM. At any rate, in reality, both effects of nonspherical deformations and volume changes of the JB are in operation.

Our self-consistent SSPJM-calculations of the energetics of metal clusters (Al, Ga, Li, Na, K, Cs) show that the total energy of a cluster is minimized for a configuration with maximum spin compensation (MSC). That is, for clusters with even number of electrons, the energy minimization gives rise to complete compensation $(N_{\uparrow} = N_{\downarrow})$, and for clusters with odd number of electrons, only one electron remains uncompensated $(N_{\uparrow} - N_{\downarrow} = 1)$. According to our calculations, the only exceptions to the MSC-rule for both neutral and ionized metal clusters (Al, Ga, Li, Na, K, Cs) of various sizes $(2 \le N \le 42)$ are Al₁₂, Al⁺₁₃, Al₁₄, and Ga₁₂. Here, N is the total number of valence electrons and N/z = n is the number of z-valent atoms in a cluster. The MSC-rule together with the monotonically increasing variation of the cluster size as a function of spin polarization give rise to the alternation of the mean distances between the nearest neighbors as a function of cluster size, N. As a result of these alternations, the total energies change, and thereby, the IPs alternate. In this work, by taking a diffusion layer for the jellium⁴³, we have also repeated our calculations for Na-clusters. Application of the diffuse-stabilized spin-polarized jellium model (dif-SSPJM) has lowered our calculated ionization energies, and as a result, we have obtained closer agreement with experimental data.

It would be interesting to compare the results of our calculations, i.e., the MSC-rule, with the results of the previous calculations in which the density parameter, r_s , was assumed to be fixed for all cluster sizes. The situation in those models is similar to that of atoms in which the external potential produced by the positive charge background with given r_s -value is fixed for different electronic configurations and only the electrons are allowed to redistribute themselves. We note that in the case of atoms, clearly the external potential due to nuclear charge remains fixed. In these cases according to the Pauli exclusion principle, electrons with parallel spins are kept apart, i.e., further apart as compared with the electrons having antiparallel spins. In fact, this is the way the electrons reduce their total electrostatic energies and this is why the electrons in a given shell assume maximum polarization consistent with the Pauli exclusion principle. In other words, the Hund's first rule is applicable in these cases. On the other hand, in the case of the SSPJM, the total energy of the system is reduced by allowing the cluster radii to expand and the ions as well as electrons to redistribute themselves. As we mentioned earlier, this results in the applicability of the MSC-rule instead of the Hund's first rule.

The organization of this paper is as follows. In section II we formulate the SSPJM, and show that in view of the Pauli exclusion principle the equilibrium bulk density parameter, r_s , for nonzero polarization is somewhat different from that of the spin-compensated system. Section III is devoted to the calculational scheme and the application of the SSPJM to metallic clusters. In section IV, we present the results of our calculations of total ground state energy per valence electron, the surface and curvature energies, the ionization potentials, and the energy second difference, $\Delta_2(N)$, which is a measure of relative stability, for different metal clusters. Lastly, we explore the condition of the equality of the Fermi energies for the up- and down-spin bands ($\varepsilon_F^{\uparrow} = \varepsilon_F^{\downarrow}$) in Appendix A.

II. THE STABILIZED SPIN-POLARIZED JELLIUM MODEL

In this section we generalize the SJM to include a uniform electron system with nonzero constant spin polarization, ζ . This formulation, in the limit of $\zeta = 0$ reduces to the SJM. The development of the formulation of the SSPJM parallels the formulation of the SJM. Here, the non-interacting kinetic energy functional, T_s , as well as the XC-energy functional, E_{xc} , depend on the polarization, ζ , of the system. But the classical Coulomb interaction of the electrons with pseudo-ions depends only on their relative distances and is independent of the spin polarization of the electrons. In a homogeneous system with nonzero electron polarization, the total electron density is the sum over the two spin density components, i.e., $n = n_{\uparrow} + n_{\downarrow}$. By defining polarization as $\zeta = (n_{\uparrow} - n_{\downarrow})/n$, each component is expressed in terms of ζ and n

$$\begin{cases} n_{\uparrow} = \frac{1}{2}(1+\zeta)n\\ n_{\downarrow} = \frac{1}{2}(1-\zeta)n. \end{cases}$$
(1)

As in the SJM, we use the Ashcroft empty core pseudopotential⁴⁴ for the interaction between an ion of charge z and an electron at a relative distance r:

$$w(r) = \begin{cases} -2z/r , & (r > r_c) \\ 0 , & (r < r_c), \end{cases}$$
(2)

where the core radius, r_c , will be fixed by setting the pressure of the system equal to zero. The average energy per valence electron in the bulk, with density n and polarization ζ , is

$$\varepsilon(n,\zeta) = t_s(n,\zeta) + \varepsilon_{xc}(n,\zeta) + \bar{w}_R(n,r_c) + \varepsilon_M(n) + \varepsilon_{bs}, \qquad (3)$$

where

$$t_s(n,\zeta) = \frac{1}{2}c_k[(1+\zeta)^{5/3} + (1-\zeta)^{5/3}]n^{2/3}$$
(4)

$$\varepsilon_{xc}(n,\zeta) = \frac{1}{2}c_x[(1+\zeta)^{4/3} + (1-\zeta)^{4/3}]n^{1/3} + \varepsilon_c(n,\zeta)$$
(5)

$$c_k = \frac{3}{5} (3\pi^2)^{2/3} \quad c_x = \frac{3}{2} \left(\frac{3}{\pi}\right)^{1/3} \tag{6}$$

All equations throughout this paper are expressed in Rydberg atomic units. Here t_s and ε_{xc} are the kinetic and exchange-correlation energies per particle respectively. For ε_c we use the Perdew-Wang parametrization⁴⁵. \bar{w}_R is the average value of the repulsive part of the pseudopotential ($\bar{w}_R = 4\pi n r_c^2$), and ε_M is the average Madelung energy of a collection of point ions embedded in a uniform negative background of density n ($\varepsilon_M = -9z/5r_0$). All nonuniformity of the true electron density $n(\mathbf{r})$ is contained in the band-structure energy ε_{bs} . r_0 being the radius of the Wigner-Seitz sphere, is given by $r_0 = z^{1/3}r_s$. We note that for monovalent metals z = 1, and if one sets $z^* = 1$ for polyvalent metals, one obtains reasonable agreement with experiment (see Ref.[33]). In the latter case, each Wigner-Seitz cell will be replaced by z smaller cells with volume $4\pi r_s^3/3$ per cell. As in the SJM, we assume that ε_{bs} is negligibly small compared to other terms in Eq. (3). Since energy, and thereby, pressure in this formalism depend on ζ as well as r_s , the stabilization of the bulk spin-polarized system with given r_s - and ζ -values, forces the pseudopotential to assume a core radius appropriate to these values, i.e., $r_c = r_c(r_s, \zeta)$. In order to stabilize a bulk system with equilibrium density \bar{n} , and constant ζ , we should set the pressure equal to zero:

$$0 = P(\bar{n},\zeta) = -\left(\frac{\partial E}{\partial V}\right)_{N,\zeta} = \bar{n}^2 \left(\frac{\partial}{\partial \bar{n}}\right)_{\zeta} \varepsilon(\bar{n},\zeta) = -\frac{1}{4\pi\bar{r}_s^2} \left(\frac{\partial}{\partial\bar{r}_s}\right)_{\zeta} \varepsilon(\bar{r}_s,\zeta).$$
(7)

This equation fixes the core radius, r_c , as a function of \bar{n} and ζ . Using

$$\left(\frac{\partial}{\partial r_s}\right)_{\zeta} t_s(r_s,\zeta) = -\frac{2}{r_s} t_s(r_s,\zeta) \tag{8}$$

and

$$\left(\frac{\partial}{\partial r_s}\right)_{\zeta} \varepsilon_x(r_s,\zeta) = -\frac{1}{r_s} \varepsilon_x(r_s,\zeta),\tag{9}$$

equation (7) results in

$$2t_s(\bar{r}_s,\zeta) + \varepsilon_x(\bar{r}_s,\zeta) - \bar{r}_s \left(\frac{\partial}{\partial \bar{r}_s}\right)_{\zeta} \varepsilon_c(\bar{r}_s,\zeta) + \frac{9}{\bar{r}_s^3} r_c^2 + \varepsilon_M(\bar{r}_s) = 0.$$
(10)

The solution of this equation at equilibrium density, \bar{n} , reduces to the following equation for r_c , which will now depend on \bar{r}_s and ζ ,

$$r_c(\bar{r}_s,\zeta) = \frac{\bar{r}_s^{3/2}}{3} \left\{ -2t_s(\bar{r}_s,\zeta) - \varepsilon_x(\bar{r}_s,\zeta) + \bar{r}_s \left(\frac{\partial}{\partial \bar{r}_s}\right)_{\zeta} \varepsilon_c(\bar{r}_s,\zeta) - \varepsilon_M(\bar{r}_s) \right\}^{1/2}.$$
 (11)

Because of the ζ -dependence of r_c , the difference potential $\langle \delta v \rangle_{\rm WS}$ becomes polarizationdependent. Here $\langle \delta v \rangle_{\rm WS}$ is the average of the difference potential over the Wigner-Seitz cell and the difference potential, δv , is defined as the difference between the pseudopotential of a lattice of ions and the electrostatic potential of the jellium positive background. As in the SJM (see Eq. (27) of Ref. [33]), at equilibrium density we have through Eq. (7)

$$\langle \delta v \rangle_{\rm WS} = \bar{n} \left[\frac{\partial}{\partial n} (\bar{w}_R(n) + \varepsilon_M(n)) \right]_{n=\bar{n}}$$
 (12)

$$= -\bar{n} \left[\left(\frac{\partial}{\partial n} \right)_{\zeta} \left(t_s(n,\zeta) + \varepsilon_{xc}(n,\zeta) \right) \right]_{n=\bar{n}}, \qquad (13)$$

so that

$$\langle \delta v \rangle_{\rm WS} = -\bar{n} \left(\frac{\partial}{\partial \bar{n}} \right)_{\zeta} \left(t_s(\bar{n}, \zeta) + \varepsilon_x(\bar{n}, \zeta) \right) + \frac{\bar{r}_s}{3} \left(\frac{\partial}{\partial \bar{r}_s} \right)_{\zeta} \varepsilon_c(\bar{r}_s, \zeta) \tag{14}$$

$$= -\frac{1}{3} \left\{ 2t_s(\bar{n},\zeta) + \varepsilon_x(\bar{n},\zeta) - \bar{r}_s \left(\frac{\partial}{\partial \bar{r}_s}\right)_{\zeta} \varepsilon_c(\bar{r}_s,\zeta) \right\}.$$
 (15)

In the above equations, $\bar{n} = 3/(4\pi \bar{r}_s^3)$ is the equilibrium electronic density of a homogeneous system which has a nonzero constant polarization. Note that, here, \bar{n} is polarizationdependent. In fact, by increasing the polarization, one increases the number of the spin-up relative to the spin-down electrons, and therefore, as a consequence of the Pauli exclusion principle, the total number of Fermi holes corresponding to the spin-up electrons is increased. This leads to the volume expansion of the system (It is a well-known fact that in a molecule, bond lengths depend on spin configurations). In order to estimate the changes of equilibrium density as a function of polarization, we put the pressure of the homogeneous spin-polarized free electron gas equal to zero. But for a homogeneous spin-polarized free electron gas with a uniform positive background, we have

$$\varepsilon(r_s,\zeta) = t_s(r_s,\zeta) + \varepsilon_x(r_s,\zeta) + \varepsilon_c(r_s,\zeta), \tag{16}$$

where the electrostatic energies have cancelled out. Now, vanishing of the pressure at equilibrium leads us to

$$0 = \frac{1}{4\pi r_s^2} \left\{ \frac{2}{r_s} t_s(r_s,\zeta) + \frac{1}{r_s} \varepsilon_x(r_s,\zeta) - \left(\frac{\partial}{\partial r_s}\right)_{\zeta} \varepsilon_c(r_s,\zeta) \right\},\tag{17}$$

the solution of which gives the equilibrium r_s as a function of ζ . At $\zeta = 0$, the latter equation yields the well-known paramagnetic value of 4.18, and therefore, in the case of non-zero polarization, it is convenient to write the equilibrium r_s -value as

$$\bar{r}_s^{\mathrm{EG}}(\zeta) = 4.18 + \Delta r_s^{\mathrm{EG}}.$$
(18)

The increment Δr_s^{EG} is used to find a rough estimate for the equilibrium r_s -values of various simple metals through

$$\bar{r}_s^{\mathcal{X}}(\zeta) = \bar{r}_s^{\mathcal{X}}(0) + \Delta r_s^{\mathrm{EG}},\tag{19}$$

where the superscript X refers to a given simple metal. In applying this result to different simple metals, we assume that this increment is independent of the value of $\bar{r}_s(\zeta = 0)$, and simply depends on the value of ζ . This is the simplest assumption we have thought of. Other forms of $\bar{r}_s^X(\zeta)$ is possible. For instance, one could use a low degree polynomial of ζ with coefficients depending on the type of metal. For Al, Ga, Li, Na, K, and Cs, $\bar{r}_s(0)$ are taken to be 2.07, 2.19, 3.28, 3.99, 4.96, 5.63 respectively. The increment of equilibrium density \bar{n} due to increasing ζ , affects the value of the core radius of the pseudopotential and causes it to increase monotonically as a function of ζ . Also the value of $\langle \delta v \rangle_{\rm WS}$ will depend on ζ . Fig. 1 shows the behavior of $\langle \delta v \rangle_{\rm WS}$ as a function of polarization, ζ , for the six metallic systems considered in here. One notes that for metals with the value of $\bar{r}_s(0)$ less than 4.18, the increase in ζ weakens the effective potential relative to its value at $\zeta = 0$, but for metals with $\bar{r}_s(0) > 4.18$, the depth of the potential increases. Once the values of $\langle \delta v \rangle_{\rm WS}$ and r_c as a function of \bar{r}_s and ζ are found, the equation (23) of Ref. [33] can be generalized to

$$E_{\text{SSPJM}}[n_{\uparrow}, n_{\downarrow}, n_{+}] = E_{\text{JM}}[n_{\uparrow}, n_{\downarrow}, n_{+}] + (\varepsilon_{M}(\bar{n}) + \bar{w}_{R}(\bar{n}, \zeta)) \int d\mathbf{r} \ n_{+}(\mathbf{r}) + \langle \delta v \rangle_{\text{WS}}(\bar{n}, \zeta) \int d\mathbf{r} \ \Theta(\mathbf{r})[n(\mathbf{r}) - n_{+}(\mathbf{r})],$$
(20)

where

$$E_{\rm JM}[n_{\uparrow}, n_{\downarrow}, n_{+}] = T_{s}[n_{\uparrow}, n_{\downarrow}] + E_{xc}[n_{\uparrow}, n_{\downarrow}] + \frac{1}{2} \int d\mathbf{r} \ \phi([n, n_{+}]; \mathbf{r})[n(\mathbf{r}) - n_{+}(\mathbf{r})], \qquad (21)$$

and

$$\phi([n, n_+]; \mathbf{r}) = \int d\mathbf{r}' \, \frac{[n(\mathbf{r}') - n_+(\mathbf{r}')]}{|\mathbf{r} - \mathbf{r}'|}.$$
(22)

 $\Theta(\mathbf{r})$ has the value of unity inside the system and zero outside. By taking the variational derivative of E_{SSPJM} with respect to spin densities $n_{\uparrow}, n_{\downarrow}$, one finds the Kohn-Sham (KS) effective potentials

$$v_{eff}^{\sigma}(\mathbf{r},\zeta) = \frac{\delta}{\delta n_{\sigma}(\mathbf{r})} (E_{\text{SSPJM}} - T_s)$$
(23)

$$=\phi([n, n_{+}]; \mathbf{r}) + v_{xc}^{\sigma}(\mathbf{r}) + \Theta(\mathbf{r}) \langle \delta v \rangle_{WS}(\bar{n}, \zeta), \qquad (24)$$

where $\sigma = \uparrow, \downarrow$. The distinction between the v_{eff}^{σ} for the two schemes of the SSPJM and the SJM is rooted in the ζ -dependence of the quantities n_+ and $\langle \delta v \rangle_{\rm WS}$ for the SSPJM. The forms of $v_{xc}^{\sigma}(\mathbf{r})$ are the same in both cases. By solving the KS-equations

$$(\nabla^2 + v_{eff}^{\sigma}(\mathbf{r}))\phi_i^{\sigma}(\mathbf{r}) = \varepsilon_i^{\sigma}\phi_i^{\sigma}(\mathbf{r}) \quad ; \quad \sigma = \uparrow, \downarrow$$
(25)

$$n(\mathbf{r}) = \sum_{\sigma=\uparrow,\downarrow} n_{\sigma}(\mathbf{r}), \qquad (26)$$

$$n_{\sigma}(\mathbf{r}) = \sum_{i(occ)} |\phi_i^{\sigma}(\mathbf{r})|^2, \qquad (27)$$

and finding the self-consistent values for ε_i^{σ} and ϕ_i^{σ} , one obtains the total energy. In the next section we apply this model to simple metal clusters.

III. CALCULATIONAL SCHEME

In the spherical-SSPJM with sharp boundary, the positive background charge density is constant and equals to $\bar{n}(\zeta)$ inside the sphere of radius $R(\zeta) = N^{1/3}\bar{r}_s(\zeta)$ and vanishes outside. In the case of dif-SSPJM, since there exists no sharp boundary for the jellium, we have taken the effective boundary at $R(\zeta) = N^{1/3}\bar{r}_s(\zeta)$. Here, for metal clusters, we take the value of ζ as

$$\zeta = (N_{\uparrow} - N_{\downarrow})/N \quad ; \quad N = N_{\uparrow} + N_{\downarrow}, \tag{28}$$

where N_{\uparrow} and N_{\downarrow} are the total numbers of valence electrons with spins up and down respectively. One could instead take ζ as the following average:

$$\bar{\zeta} = \frac{1}{\Omega} \int_0^{r_1} 4\pi r^2 \, dr \frac{[n_\uparrow(r) - n_\downarrow(r)]}{n(r)} \quad ; \quad \Omega = \frac{4\pi}{3} r_1^3, \tag{29}$$

in which r_1 is the radius at which the density components fall to the value of, say 1 percent of their peak values. In the homogeneous case, the equation for $\bar{\zeta}$ reduces to our assumed relation. The densities in the integrand of $\bar{\zeta}$ are the self-consistent values obtained by solving the KS-equations. It turns out that these values of ζ and $\bar{\zeta}$ are very close to each other and so we use the simpler one. The effective potentials in the KS-equation will be

$$v_{eff}^{\sigma}(\mathbf{r};[\bar{r}_s,\zeta]) = v_b(\mathbf{r};[\bar{r}_s]) + v_{\mathrm{H}}(\mathbf{r};[\bar{r}_s]) + v_{xc}^{\sigma}(\mathbf{r};[\bar{r}_s,\zeta]) + \Theta(\mathbf{r})\langle\delta v\rangle_{\mathrm{WS}}(\bar{r}_s,\zeta),$$
(30)

where in the case of sphere with sharp boundary,

$$v_b(r) = \begin{cases} -(N/R)[3 - (r/R)^2] ; r \le R \\ -2N/r ; r > R. \end{cases}$$
(31)

In the above equation, v_b is the potential energy of interaction between an electron and the positive charge background which depends on ζ via $r_s(\zeta)$. Also we have

$$v_{\rm H}(\mathbf{r}) = 2 \int \frac{n(\mathbf{r}')}{|\mathbf{r} - \mathbf{r}'|} d\mathbf{r}', \qquad (32)$$

$$v_{xc}^{\sigma}(\mathbf{r}) = \frac{\delta E_{xc}[n_{\uparrow}, n_{\downarrow}]}{\delta n_{\sigma}(\mathbf{r})}.$$
(33)

A spherical jellium with a finite surface thickness $(diffuse-jellium)^{43}$, is defined by

$$n_{+}(r) = \begin{cases} \bar{n}\{1 - (R+t)e^{-R/t}[\sinh(r/t)]/r\} & ; r \leq R\\ \bar{n}\{1 - ((R+t)/2R)(1 - e^{-2R/t})\}Re^{(R-r)/t}/r & ; r > R, \end{cases}$$
(34)

where $R = N^{1/3}r_s$, and t is a parameter related to the surface thickness (for other forms of diffuse-jellium see Ref.[5]). In our numerical calculations with diffuse-jellium for Na-clusters, we have chosen t = 1.0 both for neutral and singly ionized clusters. In the case of dif-SSPJM the potential energy of an electron due to the background will be

$$v_b^{dif}(r) = \begin{cases} (4\pi/3)\bar{n}(3R^2 - r^2 - 6t^2) - 8\pi\bar{n}t^2(R+t)e^{-R/t}[\sinh(r/t)]/r \; ; \; r \le R\\ -2N/r + 4\pi\bar{n}t^2[(R+t) + (R-t)e^{2R/t}]e^{-(R+r)/t}/r \; ; \; r > R. \end{cases}$$
(35)

Here, R is the effective radius of the jellium sphere, i.e., $R = N^{1/3} \bar{r}_s(\zeta)$.

IV. RESULTS AND DISCUSSIONS

In this section we discuss the calculated results for metal clusters (Al, Ga, Li, Na, K, Cs) of different sizes $(2 \leq N \leq 42)$. After computing the KS-orbitals for spin-up and spin-down components, and finding the corresponding eigenvalues, the total energy of an N-electron cluster, E(N), were calculated for both sharp- and diffuse-jellium spheres. For the sake of comparison, we have also repeated the calculations based on the JM and the SJM using the local spin density approximation (LSDA). For a given N-electron cluster, we have considered the various combinations of N_{\uparrow} and N_{\downarrow} values while keeping the total number of valence electrons, $N = N_{\uparrow} + N_{\downarrow}$, fixed.

Our calculations based on Eq. (20), show that the total energy of the system decreases as its polarization decreases, i. e., the system moves towards spin-compensated configurations. In fact, the total energy minimization is accomplished when electron spin compensation is maximum. Namely, for clusters with even number of electrons, the energy minimization gives rise to complete compensation $(N_{\uparrow} = N_{\downarrow})$, and for clusters with odd number of electrons, only one electron remains uncompensated $(N_{\uparrow} - N_{\downarrow} = 1)$.

In order to show the effect of MSC-rule, we have plotted $\Delta MSC = E_{\text{flipped}} - E_{\text{MSC}}$, as a function of N in Fig. 2 for Na- and Al-clusters. Here, E_{MSC} is the total energy of a cluster assuming MSC-configuration, and E_{flipped} is the total energy of the same cluster, but with a configuration involving only one spin-flip in the outer shells relative to the MSCconfiguration. The spin-flip is to be consistent with the Pauli exclusion principle. In fact, we have calculated ΔMSC for Al_n, Ga_n, Li_n, Na_n, K_n, and Cs_n-clusters with $2 \leq nz \leq 42$, and found that it is always positive except for Al₁₂, Al₁₃⁺, Al₁₄, and Ga₁₂. Thus, we conclude that MSC-rule is at work for nearly all clusters considered in here.

It is worth noting that in the JM and the SJM calculational schemes the minimum energy corresponds to configurations with maximum spin polarization in the outermost shells; i.e., Hund's first rule is at work. For example, in a 13-valence electron cluster, the JM and the SJM result in the minimum energy configuration in which all 5 electrons in the outermost shell (l = 2) are in parallel spin-up state $(N_{\uparrow} - N_{\downarrow} = 5)$, while in the SSPJM the energy is minimized when $N_{\uparrow} - N_{\downarrow} = 1$.

The reasons for different behaviors resulting from the use of the JM and the SJM or of the SSPJM and the dif-SSPJM, namely the applicability of the Hund's first rule or the MSC-rule lies in the unnecessary constraint of rigid jellium background assumed in earlier JMs. Note that, in these models one fixes the r_s -value for all cluster sizes with arbitrary spin configurations. Lifting such a contraint is consistent with the well-known fact that molecular bond-lengths depend on spin polarization. Moreover, from molecular dynamics calculations one can infer the alternating variation of the nearest neighbor distances as a function of cluster sizes³⁸, which supports our idea of allowing the alternating volume expansion of the jellium background positive charge distribution. In cases where the outermost shell is closed $(N = 2, 8, 18, 20, 34, 40, \ldots)$, all the four schemes of the JM, SJM, SSPJM, and dif-SSPJM predict the same spin configurations and the radius of the jellium sphere is the same for the first three schemes, but differs in the dif-SSPJM. Also, the total energy values are the same both in the SSPJM and the SJM. In cases where the outermost shell contains only one electron or lacks one electron to have a closed shell (N = 1, 3, 7, 9, 17, 19, 21, 33, 35, $39, 41, \ldots$), the above-mentioned four schemes predict the same spin configurations, but the energies are all different. Here, the difference in the SJM- and the SSPJM-values arise from different jellium radii in the two schemes for a given cluster size. In the above two special cases, the Hund's first rule and the MSC-rule are identical.

When the cluster size remains fixed while the polarization changes, as was assumed in the case of the JM and the SJM, the only way the system could reduce its total energy was to redistribute its electrons further apart. One finds the situation in the JM and the SJM to be very similar to that of atoms in which the external potential of the nucleus is kept fixed for different spin configurations. As in the case of atoms, due to the Pauli exclusion principle, parallel spin electrons are required to stay apart, i. e., further apart than when they assume a spin-compensated configuration. In the SSPJM considered in this paper, the relative positive charge background radii, $R(N,\zeta)/R(N,0)$, of clusters are allowed to expand with increasing polarization. In a sense, here, the ionic motions are simulated through such an expansion. Now, because of the above-mentioned freedom, as soon as electrons try to take advantage of the Pauli exclusion principle and begin to spill out of the cluster, the positive charge background will try to follow them. In other words, the freedom of cluster size expansion renders the application of Hund's first rule unnecessary, and the SSPJM chooses to be in a spin-compensated configuration. In short, contrary to the case of the spherical-JM and the spherical-SJM, which are governed by the Hund's first rule, here the MSC-rule is in effect, and it is this MSC effect which results in the changes in the level separations near the Fermi level for neutral and ionized clusters, and thereby, gives rise to the well-known odd-even alternations in IPs of alkali metal clusters. One notes that our viewpoints about the changes in level separations, and those that attribute this effect to nonspherical shape deformations refer to two complementary effects. That is, in our case, the shape has remained spherical whereas the volume is allowed to change, but in the case of deformed-JMs, the volume is fixed and the shape is allowed to change. In a combined effect, one allows, at the same time, the volume of a cluster to change and its shape to deform.

The size of jellium sphere in the SSPJM for neutral and singly ionized clusters are different. This should be contrasted with the cases of the JM and the SJM in which the sizes for the neutral and ionized clusters are assumed to be the same. Our self-consistent calculations show that the polarization ζ , for metal clusters in their minimum energy configuration as a function of total number of valence electrons, N, satisfies (with exceptions for Al₁₂, Al⁺₁₃, Al₁₄, Ga₁₂) the following equation:

$$\zeta(N) = \frac{[1 - (-1)^N]}{2N} = \begin{cases} 0 \ ; N \text{ even} \\ 1/N \ ; N \text{ odd.} \end{cases}$$
(36)

Using the above equation for polarization, we plot the equilibrium r_s -value for different Na-clusters in Fig. 3. As seen from the figure, for an Na-cluster with even number of atoms, r_s equals 3.99 and with odd number of atoms the envelope is a decreasing function of N. According to Eq. (19), Fig. 3 for other metals remains the same but shifted according to the value of $r_s(0)$. As is expected, in the limit of large-N clusters, addition or removal of an electron does not change the configurations of all other ions. Comparing Fig. 3 with Fig. 15(a) of Ref. [38] for average nearest neighbor distances, one notes the same staggering effect.

Fig. 4a and Fig. 4b show the values of the nonbulk binding energies, $E/N - \alpha_V$, for Na- and Al-clusters using the JM, the SJM, and the SSPJM along with the LSDA. Here,

 α_V represents the bulk binding energy. The calculated energies based on the JM, the SJM, and the SSPJM for Na-clusters, aside from the details, are nearly close and positive as expected. This is because the sodium r_s -value (3.99) is close to the zero-pressure jellium r_s -value (4.18). However, in the case of Al-clusters, the energies based on the SJM and the SSPJM remain near each other and are positive, but the energies based on the JM is considerably away from them and at times assume negative values (see Fig. 4b). The reason is that the JM at high densities fails (note that the r_s -value of Al is 2.07) and leads to mechanical instability. We have also calculated the nonbulk binding energies of other metal clusters (Ga, Li, K, Cs) and see that as r_s decreases, the energies based on the JM moves away from the results based on the SJM and the SSPJM. By looking at Fig. 1 we note that the $\langle \delta v \rangle_{\rm WS}$ contribution to the total energies are positive in the case of Cs and K (for which $r_s > 4.18$); and negative in the case of Al, Ga, Li, and Na (for which $r_s < 4.18$). Thus, in the case of K- and Cs-clusters we should expect that the JM energies using the LSDA lie above the SJM- and the SSPJM-energies, and in the case of Na-, Li-, Ga-, and Al-clusters we should expect it to lie below them. Our calculations of the nonbulk energies of Al-, Ga-, Li-, Na-, K-, Cs-clusters confirm these conclusions.

In Fig. 5 we show the plot of $\Delta_2(N) = E(N+1) + E(N-1) - 2E(N)$ which determines the relative stability of different Na-clusters. We have also calculated $\Delta_2(N)$ for other metal clusters mentiond in this paper. In the plot using the SSPJM, the incorrect peaks predicted by the spherical-SJM at N = 5, 13, 27, 37 have disappeared and the clusters with N = 8, 18, 20, 40 are predicted to be more stable. These results are consistent with the fine-structure observed experimantally in the abundance curve⁴. Similar observations can be made from the plots of $\Delta_2(N)$ for other metals considered in here. The overall agreement between our results and experimental data is good.

Next, we have calculated the surface and curvature energies of Al-, Ga-, Li-, Na-, K-, Cs-clusters. According to the liquid drop model^{46,47,18}, one may write the total energy of a finite quantal system in the form of

$$E = \overline{E} + \delta E \tag{37}$$

where δE is shell correction and \overline{E} is the smooth part of the total energy which is written as a sum of volume, surface, and curvature contributions. In the case of spherical geometry, \overline{E} reduces to the following parametrized equation as a function of the number of valence electrons in a neutral cluster

$$\overline{E}(N) = \alpha_V N + \alpha_S N^{2/3} + \alpha_C N^{1/3}.$$
(38)

Here, α_V is the total energy per electron in the bulk. Its absolute values for the metals Al, Ga, Li, Na, K, Cs using the SJM or the SSPJM are respectively 10.57, 10.14, 7.37, 6.26, 5.18, 4.64 in units of electron-volts using the r_s -values mentioned earlier. The surface energy, σ , and the curvature energy, A_C , are related to the parameters α_S and α_C through the relations:

$$\sigma = \frac{1}{4\pi r_s^2} \alpha_S, \qquad A_C = \frac{1}{4\pi r_s} \alpha_C. \tag{39}$$

The parameters α_S and α_C are obtained by a least-square fit of our self-consistent total energies to Eq. (38).

Fig. 6a shows the surface energies of different metals as a function of their r_s -values for the three schemes using the SSPJM, the SJM, and the JM, and compared with the results obtained by others (BULK)⁴⁸. The surface energies of the SSPJM and the SJM remain positive for the metals considered here, but it becomes negative in the case of the JM (as mentioned in the introduction) for high electron density metals (Al, Ga).

Fig. 6b shows the curvature energies of various metals as a function of their r_s -values. The SSPJM results in a higher curvature energies than the other two schemes using the SJM and the JM. The results of bulk calculations⁴⁸ are also shown.

Finally, in Figs. 7a-f, we have compared the ionization energies of metal clusters for different schemes as well as with the experimental values. The ionization energy of an Nvalence electron cluster is defined as the difference between the total ground state energy of that system with N and (N-1) valence electrons. The experimental values are taken from Ref. [49] for aluminum, Ref. [4] for lithium, sodium, and potassium. When we calculate the IPs by means of the SSPJM and the SJM, we see that the odd-even alternations in alkali metal clusters, not present in the results of the JM or the SJM results, show themselves up in the SSPJM calculations. In the SJM using the LSDA, kinks appear only at half-filled and closed shells, whereas in both the SSPJM and the dif-SSPJM, there exists a peak at the middle of each pair of adjacent odd numbers. These peaks correspond to clusters with even number of atoms, in agreement with experimental data. In dif-SSPJM, the ionization energies of Na-clusters are lowered so that the values near the closed shells (where the nonsphericity becomes less important) are in good agreement with experiment than the corresponding values of the other two models. At the end, because of the assumed spherical geometry, the pronounced shell effects are still present in the IPs when we go from one closed shell cluster to a cluster with one more electron and the overall saw-toothed behavior of IPs remains. In other metals the agreement between theory and experiment is poor for all the three schemes. We think our results for Na-clusters will improve if dif-SSPJM is used along with spheroidal or ellipsoidal geometries.

V. SUMMARY AND CONCLUDING REMARKS

In this paper, we have generalized the SJM to the spin-polarized case by allowing the volume of the spherical positive charge background to change and have calculated the energetics of metal clusters (Al, Ga, Li, Na, K, Cs). Our self-consistent calculations show that for spherical geometries, the minimum-energy of a metal cluster is obtained when the electronic spin compensation is maximum. That is, in contrast to the spherical-JM and the spherical-SJM which are governed by the Hund's first rule, here the MSC-rule is in effect. We have discussed in detail that the situations in the JM and the SJM are similar to that in atoms. In both cases, the external potential – being due to the positive charge background or due to the nuclear charge – are fixed and therefore, in both cases the Hund's first rule is applicable. However, in the case of the SSPJM, because of the extra degrees of freedom, namely the expansion of the positive charge background, the system assumes maximum spin-compensated configurations. This MSC-rule results in the alternations of the average distance between the nearest neighbors, and thereby, in the alternations of the IPs. Moreover, application of the dif-SSPJM for alkali metal clusters brings the IP-values closer to the experimental data. Finally, we believe that if the SSPJM is used in conjunction

with nonspherical shape deformations, better agreements between theory and experiment will result.

ACKNOWLEDGEMENT

M.P. is indebted to John P. Perdew for his helpful comments, and also Erick Koch for the discussion. N.N. would like to thank N. H. March and U. Röthlisberger for their helpful discussions. The authors would like to acknowledge the International Center for Theoretical Physics, Trieste, Italy, for their warm hospitality.

APPENDIX A: STABILITY CONDITIONS IN A SPIN-POLARIZED INFINITE JELLIUM

In an unpolarized infinite jellium ($\zeta = 0$), the stability of the system is obtained via $\partial \varepsilon / \partial r_s |_{\zeta=0} = 0$. In other words, in this case, it suffices to establish mechanical stability. This is done by employing the Ashcroft empty-core pseudopotential whose core radius is fixed by setting the pressure equal to zero. However, for a spin-polarized infinite jellium, the total energy per electron, ε , depends on n and ζ . Thus

$$d\varepsilon = \left(\frac{\partial\varepsilon}{\partial n}\right)_{\zeta} dn + \left(\frac{\partial\varepsilon}{\partial\zeta}\right)_n d\zeta.$$
(A1)

At equilibrium, the following two equations must be satisfied:

$$\left(\frac{\partial\varepsilon}{\partial n}\right)_{\zeta} = 0 \tag{A2}$$

$$\left(\frac{\partial\varepsilon}{\partial\zeta}\right)_n = 0. \tag{A3}$$

Eq. (A2) establishes the mechanical stability and Eq. (A3) sets the Fermi energy of the upand down-spin bands equal, i. e., $\varepsilon_F^{\uparrow} = \varepsilon_F^{\downarrow}$. The latter point is proved below. ε_F^{\uparrow} is the highest occupied spin-up KS-level and $\varepsilon_F^{\downarrow}$ is the highest occupied spin-down KS-level. **proof:**

Following the work of Russier, Salahub, and Mijoule⁵⁰, we can write

$$\left(\frac{\partial\varepsilon}{\partial\zeta}\right)_{n} = \frac{\partial\varepsilon}{\partial n_{\uparrow}} \left(\frac{\partial n_{\uparrow}}{\partial\zeta}\right)_{n} + \frac{\partial\varepsilon}{\partial n_{\downarrow}} \left(\frac{\partial n_{\downarrow}}{\partial\zeta}\right)_{n}, \tag{A4}$$

so that using Eq. (1) reduces to

$$\left(\frac{\partial\varepsilon}{\partial\zeta}\right)_n = \frac{1}{2}n\left(\frac{\partial\varepsilon}{\partial n_{\uparrow}} - \frac{\partial\varepsilon}{\partial n_{\downarrow}}\right). \tag{A5}$$

Now, using the variational principle for the ground state energy of a homogeneous system subject to the two constrains

$$\int n_{\sigma} d\mathbf{r} = N_{\sigma}, \qquad \sigma = \uparrow, \downarrow, \qquad (A6)$$

we have

$$\delta \left\{ \int (n_{\uparrow} + n_{\downarrow}) \varepsilon(n_{\uparrow}, n_{\downarrow}) d\mathbf{r} - \mu_{\uparrow} \int n_{\uparrow} d\mathbf{r} - \mu_{\downarrow} \int n_{\downarrow} d\mathbf{r} \right\} = 0.$$
 (A7)

This equation results in the following Euler equations:

$$\varepsilon + n \frac{\partial \varepsilon}{\partial n_{\uparrow}} - \mu_{\uparrow} = 0, \tag{A8}$$

$$\varepsilon + n \frac{\partial \varepsilon}{\partial n_{\downarrow}} - \mu_{\downarrow} = 0. \tag{A9}$$

Subtracting Eq. (A9) from Eq. (A8) and dividing both sides by n, one obtains

$$\left(\frac{\partial\varepsilon}{\partial n_{\uparrow}} - \frac{\partial\varepsilon}{\partial n_{\downarrow}}\right) = \frac{1}{n}(\mu_{\uparrow} - \mu_{\downarrow}). \tag{A10}$$

Substituting Eq. (A10) into Eq.(A5), one obtains

$$\left(\frac{\partial\varepsilon}{\partial\zeta}\right)_n = \frac{1}{2}(\mu_{\uparrow} - \mu_{\downarrow}). \tag{A11}$$

Eqs. (A11) and (A3) in conjunction with Koopmans' theorem⁵¹ entails the equality of the two Fermi levels for an infinite homogeneous spin-polarized jellium.

However, in this paper we have calculated the total energy of finite clusters. In such systems, because of the discrete nature of the energy eigenvalues, the equality of the spinup and spin-down Fermi energies does not hold any more. Thus, the stabilization will be established through Eq. (A2) and when $\partial E/\partial \zeta |_{r_s}$ changes sign. In practice, for a given ζ , we have first calculated the core radius entering the Ashcroft pseudopotential via Eq. (11) and used it as an input for the total energy calculation of the cluster. We then, varied ζ , i. e., the cluster's spin configuration, till total energy minimization was attained. Although, the procedure employed here is a consistent choice, but one could start with a two parameter pseudopotential and apply Eq. (A2) and Eq. (A3) to the stabilized spin-polarized infinite jellium. In this way, one obtains the dependence of the two mentioned parameters on ζ and r_s and repeats the clusters' total energy calculations again. Work in this direction is in progress.

REFERENCES

- ¹ W. E. Ekardt, Phys. Rev. B**29**, 1558 (1984).
- ² W. D. Knight, K. Clemenger, W. A. de Heer, W. A. Saunders, M. Y. Chou, and M. L. Cohen, Phys. Rev. Lett. **52**, 2141 (1984).
- ³ W. A. de Heer, W. D. Knight, M. Y. Chou, and M. L. Cohen, 1987 in Solid State Physics, Vol 40, edited by H. Ehrenreich and D. Turnball (Academic, New York) p. 93
- ⁴ W. A. de Heer, Rev. Mod. Phys. **65**, 611 (1993) and references therein.
- ⁵ M. Brack, Rev. Mod. Phys. **65**, 677 (1993) and references therein.
- ⁶C. Yannouleas and Uzi Landman, Phys. Rev. B48, 8376 (1993).
- ⁷ P. Hohenberg and W. Kohn, Phys. Rev. **136**, B864 (1964).
- ⁸ W. Kohn and L. J. Sham, Phys. Rev. **140**, A1133 (1965).
- ⁹ R. G. Parr and W. Yang, *Density Functional Theory of Atoms and Molecules*, Oxford University Press, New York 1989, and references therein.
- ¹⁰ R. M. Dreizler and E. K. U. Gross, *Density Functional Theory*, Springer Verlag, Berlin 1990, and references therein; *Density Functional Theory*, Edited by E. K. U. Gross and R. M. Dreizler, Plenum Publishing Corporation, New York (1995).
- ¹¹ K. Clemenger, Phys. Rev. B**32**, 1359 (1985).
- ¹² W. Ekardt and Z. Penzar, Phys. Rev. B38, 4273 (1988).
- ¹³ W. Ekardt and Z. Penzar, Phys. Rev. B43, 1322 (1991).
- ¹⁴ Z. Penzar and W. Ekardt, Z. Phys. D17, 69 (1990).
- ¹⁵G. Lauritsch, P. -G. Reinhard, J. Meyer, and M. Brack, Phys. Lett. A160, 179 (1991).
- ¹⁶ T. Hirschmann, M. Brack, and J. M. Meyer, Ann. Phys. (Leipzig) **3**, 336 (1994).
- ¹⁷C. Kohl, B. Montag, and P. -G. Reinhard, Z. Phys. D35, 57 (1995).
- ¹⁸ C. Yannouleas and Uzi Landman, Phys. Rev. B**51**, 1902 (1995).
- ¹⁹ V. Bonacic-Koutecky, P. Fantucci, and J. Koutecky, Phys. Rev. B37, 4369 (1988).
- ²⁰ M. Koskinen, P. O. Lipas, and M. Manninen, Z. Phys. D35, 285 (1995).
- ²¹ N. D. Lang and W. Kohn, Phys. Rev. B1, 4555 (1970).
- ²² N. W. Ashcroft and D. C. Langreth, Phys. Rev. **155**, 682 (1967).
- ²³ N. D. Lang and W. Kohn, Phys. Rev. B**3**, 1215 (1971).
- ²⁴ M. Manninen, Phys. Rev. B**34**, 6886 (1986).
- ²⁵ W. -D. Schöne, W. Ekardt, and J. M. Pacheco, Phys. Rev. B**50**, 11079 (1994).
- ²⁶ R. Monnier and J. P. Perdew, Phys. Rev. B17, 2595 (1978).
- ²⁷ R. Monnier and J. P. Perdew, D. C. Langreth, and J. W. Wilkins, Phys. Rev. B18, 656 (1978).
- ²⁸ V. Sahni, J. P. Perdew, and J. Gruenebaum, Phys. Rev. B23, 6512 (1981).
- ²⁹ C. A. Utreras-Diaz and H. B. Shore, Phys. Rev. Lett. **53**, 2335 (1984).
- ³⁰ H. B. Shore and J. H. Rose, Phys. Rev. Lett. **66**, 2519 (1991).
- ³¹ J. H. Rose and H. B. Shore, Phys. Rev. B43, 11605 (1991).
- ³² C. A. Utreras-Diaz and H. B. Shore, Phys. Rev. B40, 10345 (1989).
- ³³ J. P. Perdew, H. Q. Tran, and E. D. Smith, Phys. Rev. B42, 11627 (1990).
- ³⁴C. Fiolhais, J. P. Perdew, S. Q. Armster, J. M. MacLaren, and M. Brajczewska, Phys. Rev. B51, 14001 (1995).
- ³⁵ M. Brajczewska, C. Fiolhais, and J. P. Perdew, Int. J. Quantum Chem. Quantum Chem. Symp. 27, 249 (1993).

- ³⁶ P. Ziesche, M. J. Puska, T. Korhonen, and R. M. Nieminen, J. Phys.: Condens. Matter 5, 9049 (1993).
- ³⁷ H. A. Jahn and E. Teller, Proc. R. Soc. London Ser. A **161**, 220 (1937).
- ³⁸ U. Röthlisberger and W. Andereoni, J. Chem. Phys. **94**, 8129 (1991).
- ³⁹ R. Car and M. Parrinello, Phys. Rev. Lett. **55**, 2471 (1985).
- 40 M. Payami and N. Nafari, ICTP-Preprint: IC/95/262.
- ⁴¹ M. M. Kappes, M. Schär, U. Röthlisberger, C. Yeretzian, and E. Schumacher, Chem. Phys. Lett. **143**, 251 (1988).
- ⁴² M. L. Homer, J. L. Persson, E. C. Honea, and R. L. Whetten, Z. Phys. D22, 441 (1991).
- ⁴³ A. Rubio, L. C. Balbás, and J. A. Alonso, Z. Phys. D19, 93 (1991).
- ⁴⁴ N. W. Ashcroft, Phys. Lett. **23**, 48 (1966).
- ⁴⁵ J. P. Perdew and Y. Wang, Phys. Rev. B45, 13244 (1992).
- ⁴⁶ M. Brack, Phys. Rev. B **39**, 3533 (1989).
- ⁴⁷ E. Engel, J. P. Perdew, Phys. Rev. B43, 1331 (1991).
- ⁴⁸ C. Fiolhais and J. P. Perdew, Phys. Rev. B **45**, 6207 (1992).
- ⁴⁹ K. E. Schriver, J. L. Persson, E. C. Honea, and R. L. Whetten, Phys. Rev. Lett. **64**, 2539 (1990).
- ⁵⁰ V. Russier, D. R. Salahub, and C. Mijoule, Phys. Rev. B42, 5046 (1990).
- ⁵¹ T. C. Koopmans, Physica 1, 104 (1933); and *Theory of The Inhomogeneous Electron Gas*, Edited by S. Lundqvist and N. H. March, Plenum Press, New York, page 142 (1984).

FIGURES

FIG. 1. Equilibrium potential difference in Rydbergs versus polarization for Al, Ga, Li, Na, K, and Cs metals.

FIG. 2. The behavior of Δ MSC as a function of number of valence electrons, N, in units of eV. Both neutral and singly ionized metal clusters (Al and Na) are presented. Δ MSC is the difference between the energy of the maximum spin compensated electronic configuration from the energy of a different configuration in which one electron is flipped. In the case of Na-clusters all Δ MSCs are positive and in the case of Al-clusters, except for Al₁₂, Al₁₃⁺, Al₁₄, all Δ MSCs are again positive.

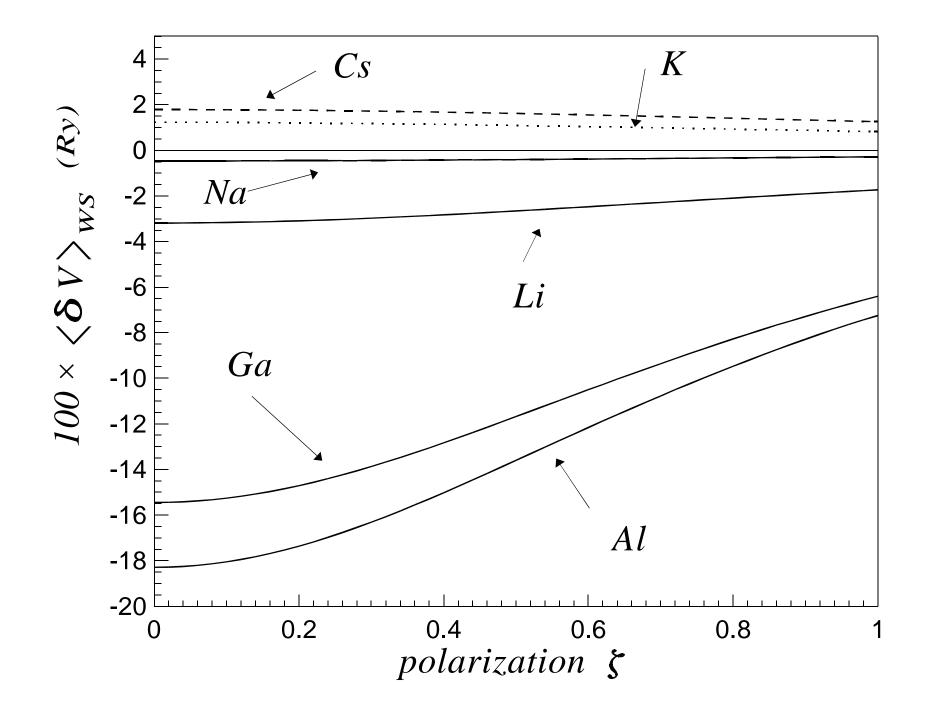
FIG. 3. Equilibrium Wigner-Seitz radius in atomic units as a function of number of atoms in an Na-cluster.

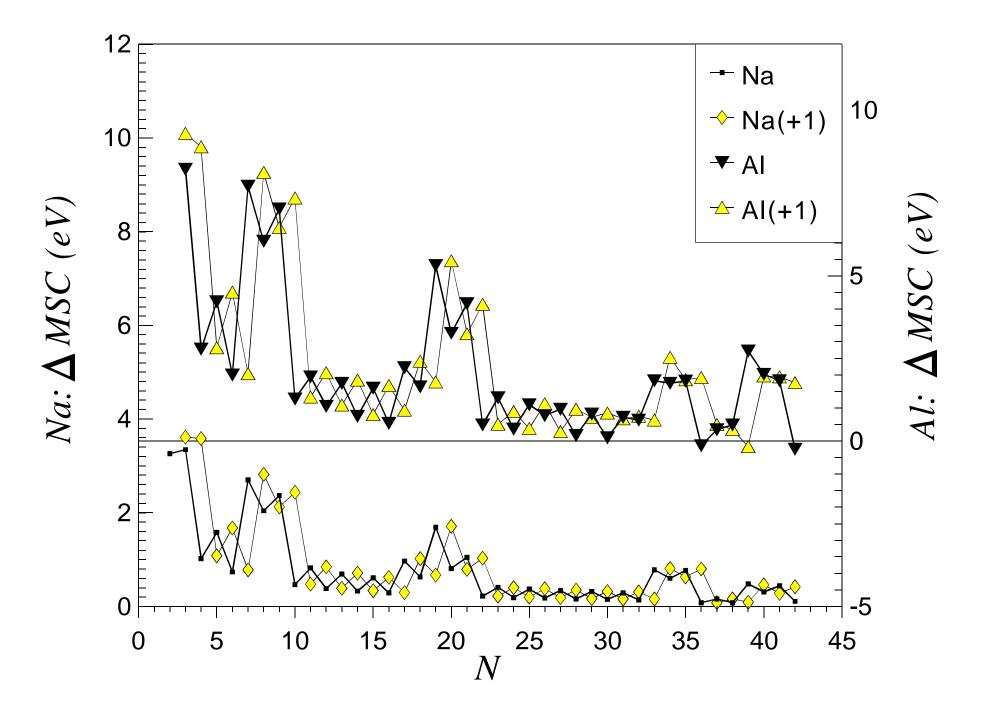
FIG. 4. The nonbulk total energies per atom of (a) Na- and (b) Al-clusters as a function of number of valence electrons in the cluster. The symbols, solid squares, diamonds, and triangles correspond to the SSPJM, the SJM, and the JM respectively. For Al, the physical points (i.e., multiples of 3) are specified and for Na, the large square symbol corresponds to dif-SSPJM.

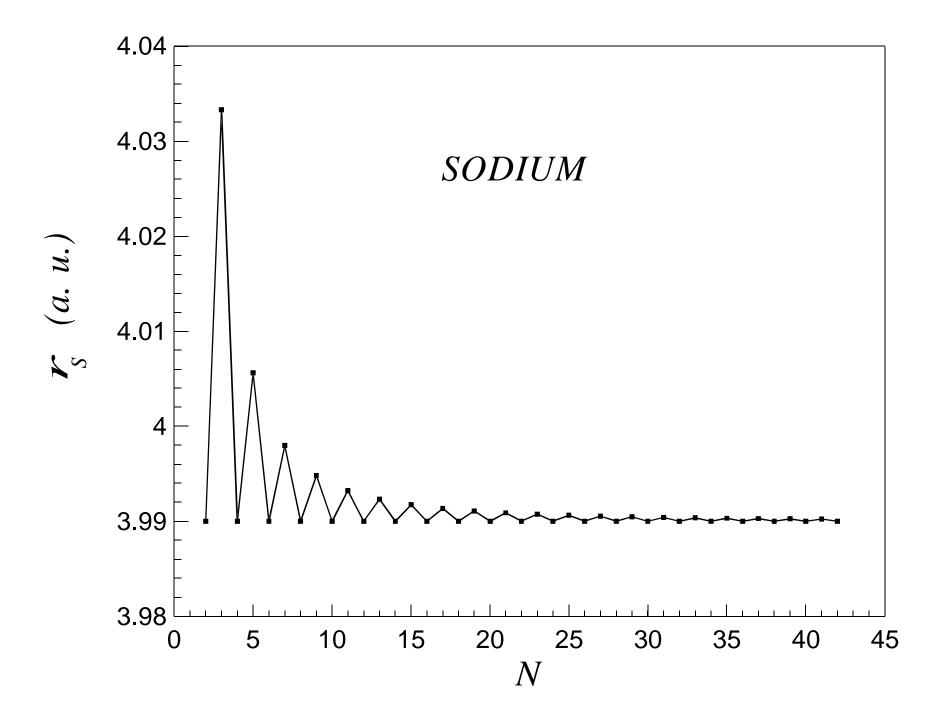
FIG. 5. The second difference of total energies of Na-clusters in units of eV as a function of number of atoms in a cluster. The symbols, solid squares, triangles, and diamonds correspond to SJM, JM, and dif-SSPJM respectively.

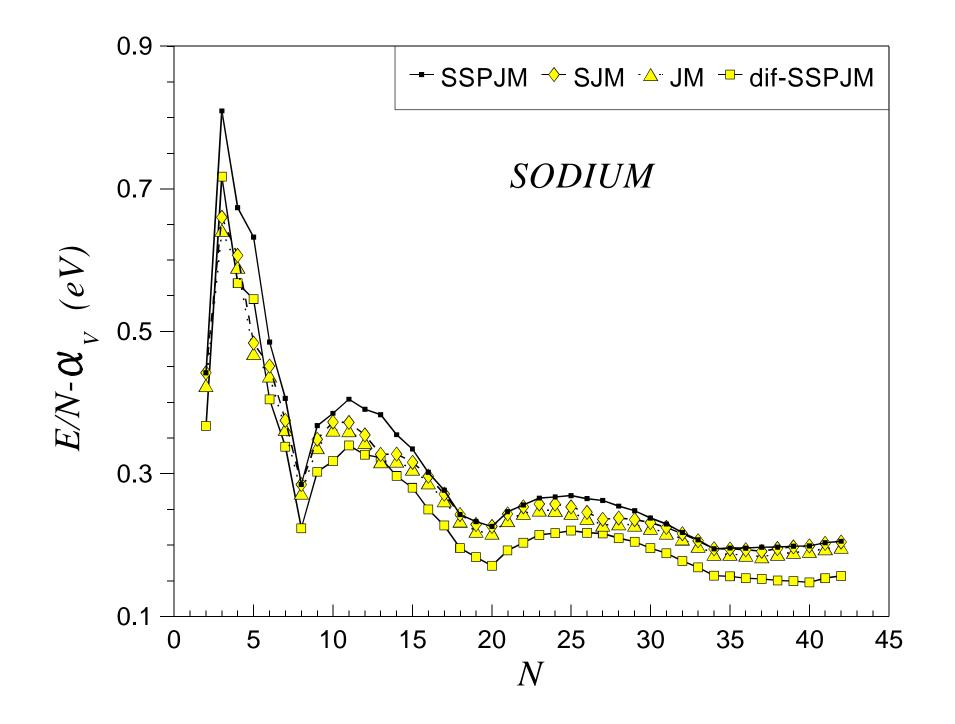
FIG. 6. (a) Surface energies of metals, σ , as a function of their r_s -values, in units of erg/cm²; (b) Curvature energies of metals, A_c , as a function of their r_s -values, in units of mili-hartree/bohr. The symbols, crosses, solid squares, triangles, and upside-down triangles correspond to the SSPJM, SJM, JM, and bulk calculations (BULK) (see Ref. [48]). The negative surface energies of Al and Ga are due to the instability of the JM.

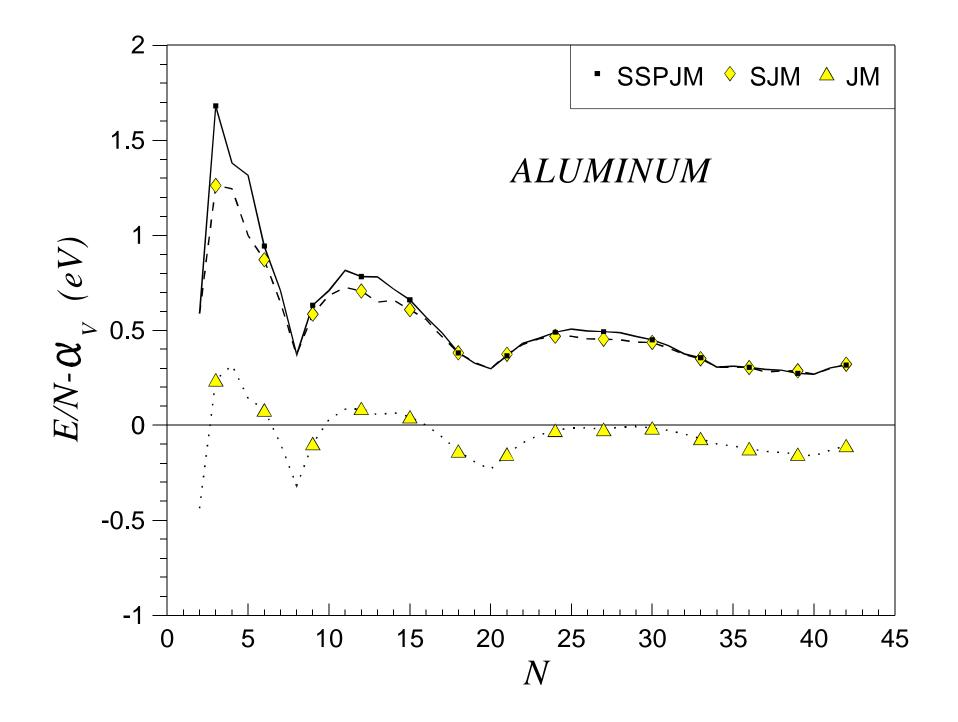
FIG. 7. The ionization energies in units of eV as a function of the number of atoms in a cluster for (a) Al, (b) Ga, (c) Li, (d) Na, (e) K, (f) Cs. The large solid squares represent the experimental data. The small solid squares, the diamonds, the triangles, and the upside-down triangles, respectively correspond to calculational schemes based on the SSPJM, the SJM, the JM, and the dif-SSPJM. By moving towards closed shell electronic structures, the agreement between the results of the dif-SSPJM and experimental data improves.

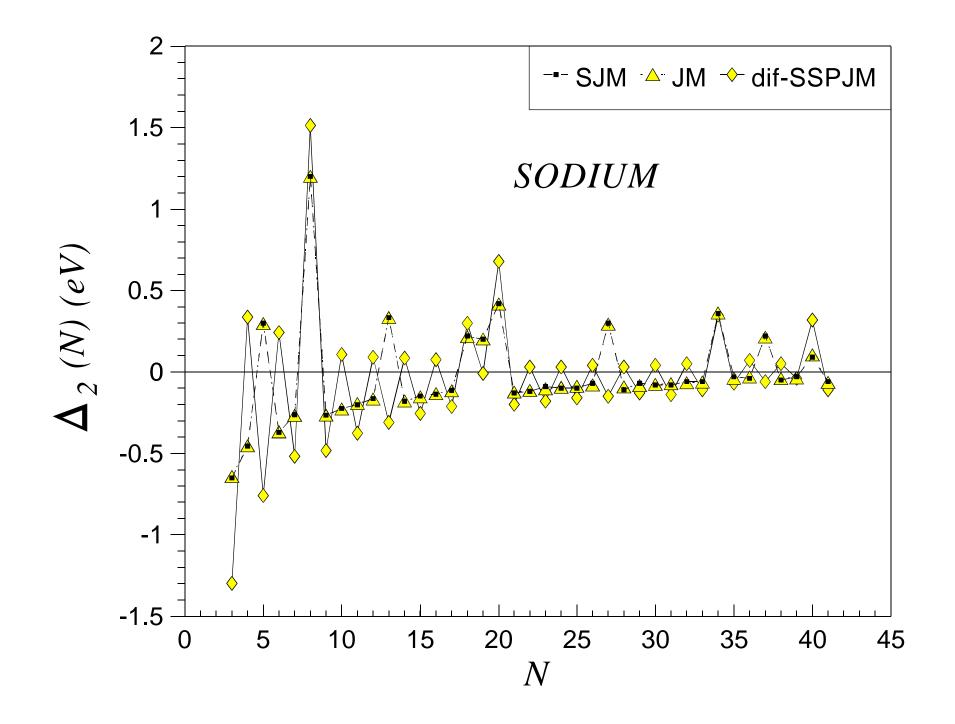


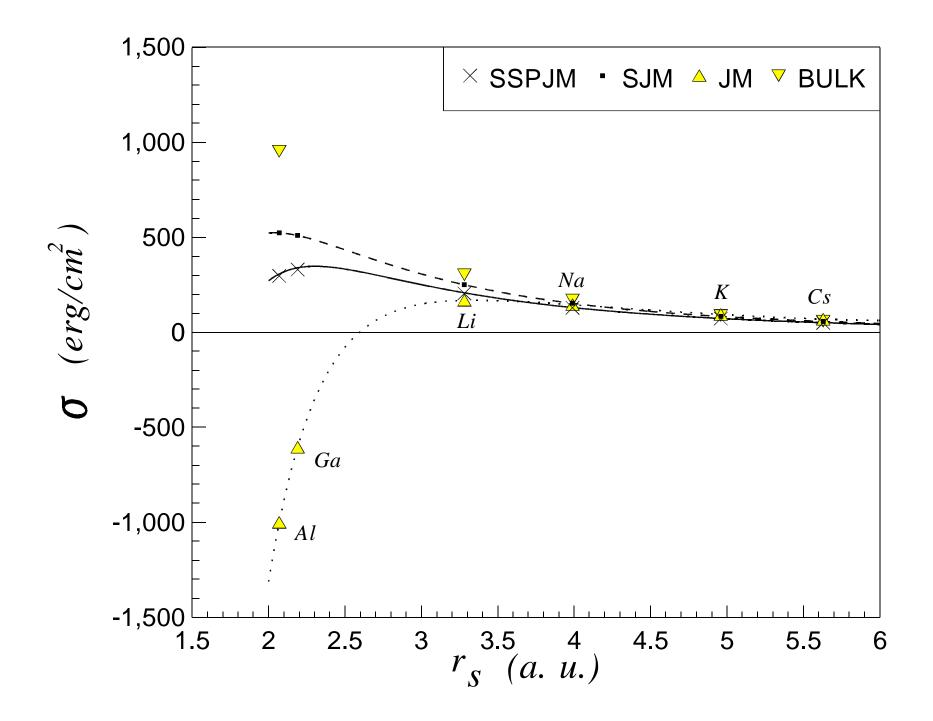


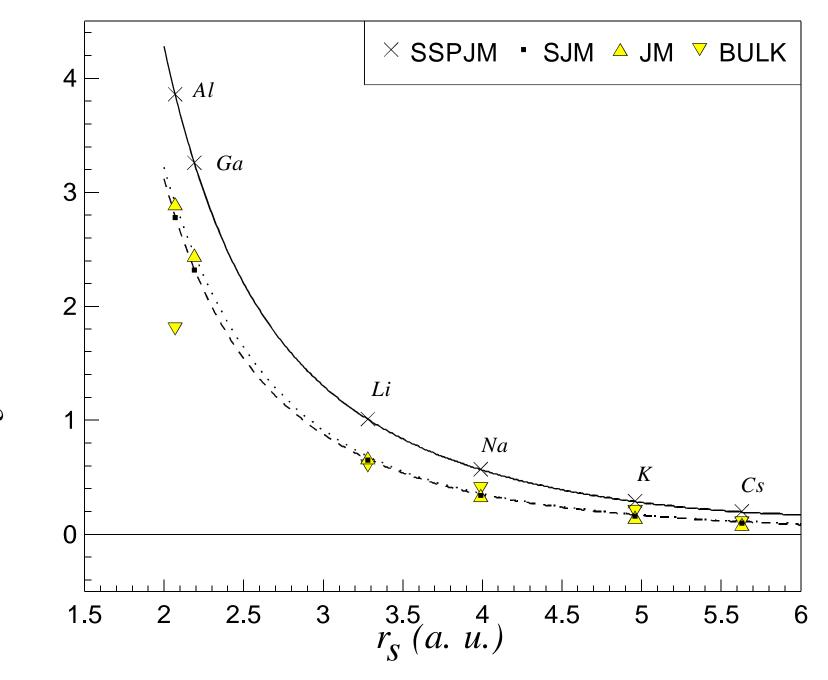












 A_c (mhartree/bohr)

